Bandlimited impedance inversion: using well logs to fill low frequency information in a non-homogenous model

Heather J.E. Lloyd and Gary F. Margrave

ABSTRACT

An acoustic bandlimited impedance inversion study was done to compare the results obtained when the baseline log; or alternatively, a monitor log are used to provide the low frequency information for the inversion. The model was created using the baseline log for the regional trend and placing the fluid substituted (monitor) log at the injection site in the center of the section. These wells were then interpolated along a geological section with a 2.8 degree regional dip. This impedance section was then converted to reflectivity and convolved with a zero phase, Ormsby wavelet to create a normal incident synthetic data set. The frequency spectrum of the logs and synthetic data were compared to find a suitable low frequency cut-off value. The low cut-off value of 4.5 Hz was chosen as frequencies higher than this were found to produce low frequency smearing across the section. The inversions were carried out using this low frequency cut-off for the logs and the high frequency cut-off for the seismic data was set at 85 Hz. The baseline inversion had a mean error of 28% at the injection site where the monitor inversion had an error of 23%. Both inversions had a regional error of ±10% when compared to the true impedance given by the model. The cross-correlation between the seismic data and the synthetic seismogram for the monitor inversion case was higher, and the sum of the error between the true impedance and the monitor inversion was slightly lower when compared with the baseline inversion. This shows that the monitor inversion is slightly better than the baseline inversion. It was found that more testing is required, using different models and acquisition geometries to determine which log is better to use in time-lapse studies. The findings of this paper suggest that possibly the best results can be obtained when the baseline log is used for the regional area and the monitor log is used for the injection area.

INTRODUCTION

Time-lapse seismic surveys are being conducted more often as the need to monitor fluids in reservoirs increases. While the actual seismic data can be used to see differences in the reservoir, acoustic impedance is a better indicator of changes as it has higher resolution than the seismic data (Pendrel, 2006) and is a measurement of the actual properties of the layers where as seismic data only indicates the contrast between layers at their boundaries. This enables fluid changes in the reservoir to be more easily identified in the seismic data and the monitoring of fluid migration more successful. Acoustic impedance has been used as a method for retrieving rock properties since the late 1970's(Lindseth, 1979). One method of retrieving the acoustic impedance from the seismic data is the bandlimited impedance inversion approach. Inherently, seismic data is missing low frequency data which must be supplied by other means for the algorithm to work. Lindseth (1979) suggested that information from a nearby well log could be used to provide this missing low-frequency component. This paper compares acoustic bandlimited impedance inversions when using a baseline log, recorded before fluid

injection and a monitor log, recorded after the fluid injection, to see if there is a significant benefit to using one or the other.

This study uses data from Violet Grove in the Pembina Oil Field, located in the west-central plains of Alberta (McCrank, 2009). Other impedance studies have been done in the Pembina Oil field such as the study by McCrank (2009) at Alder Flats was conducted for an enhanced coal bed methane production project by injecting carbon dioxide into the formation. A time-lapse seismic survey was conducted and the low resolution of the seismic data was not able to indicate the extent of the carbon dioxide plume. An acoustic impedance inversion was then calculated and a lower impedance anomaly was noticed in the time lapse inversion data. This anomaly was consistent in size with the amount of carbon dioxide that was injected into the coal beds. This example shows that acoustic impedance inversion is extremely useful for monitoring fluids in a reservoir.

This paper will explain the theory behind bandlimited acoustic impedance. The Violet Grove model used throughout this paper will be discussed. The results using the modified BLIMP algorithm written in MATLAB and results obtained using Hampson Russell software will be compared. Conclusions will then be drawn and future work will then be discussed.

THEORY

Noise free seismic data can described using the convolutional model

$$s(t) = r(t) * w(t), \tag{1}$$

where s(t) is the signal, r(t) is the reflectivity sequence and w(t)is the wavelet.. Acoustic impedance is defined as the product of the density and the velocity of a layer. Reflectivity is related to acoustic impedance by

$$r_{j+1} = \frac{I_{j+1} - I_j}{I_{j+1} + I_j}, \tag{2}$$

where I_j is the impedance for the j_{th} layer. This result can be rearranged as

$$I_{j+1} = I_j \frac{1+r_j}{1-r_j} = I_1 \prod_{k=1}^{j} \frac{1+r_k}{1-r_k}, \tag{3}$$

which gives impedance in terms of reflectivity, where I_1 is the impedance at the surface. If we can remove the wavelet from the data perfectly by deconvolution, the deconvolved data is the reflectivity. If these assumptions hold then Equation 3 is also the recursion formula to estimate impedance from the reflectivity (Oldenburg et al., 1983). If we take the limit of Equation 2 for a continuous case we get

$$\mathrm{r(t)} = \lim_{\Delta t \to 0} \frac{I(t) - I(t-\Delta t)}{I(t) + I(t-\Delta t)} = \frac{d\left({}^{I(t)}/_{I_o}\right)}{2\left({}^{I(t)}/_{I_o}\right)}, \tag{4}$$

where I_o, is the impedance at the surface. We can recognize the right-hand side of Equation 4 as the differential of the logarithm of impedance so

$$r(t) = \frac{1}{2} d[ln(I(t)/I_o)], \quad (5)$$

where the higher terms can be disregarded as long as the reflectivity coefficients are less than 0.3 (e.g. Oldenburg et al., 1983). This result can then be solved for impedance

$$I(t) = I_o e^{2\int_0^t r(\tau)}, \quad (6)$$

which shows that impedance can be estimated by integrating the deconvolved trace, then exponentiation, and finally scaling by "I_o"..

An inherent problem when applying this method of acoustic impedance inversion to seismic data is that the data is bandlimited. This problem is a result of a reflectivity sequence being convolved with a bandlimited wavelet. The wavelet is bandlimited in practice as the earth attenuates high frequencies, some seismic sources are not capable of producing low frequencies and only special geophones are capable of reliably recording the low frequencies at the surface. The low frequencies (0-5 Hz) that are not present in seismic data are essential for creating the character or scale of the impedance log (Lindseth, 1979) where as the higher frequencies are responsible for contributing to the detail of the impedance log. When these low frequencies are not present in the seismic data, they can be introduced as an auxiliary dataset.. In this study, these low frequencies come from a well log near the seismic acquisition site (as suggested by Lindseth, 1979). This required a decision to be made to choose a cut-off frequency, below which the log data are used and above which the seismic data are used. This study will investigate an appropriate low frequency cut-off that should be applied to the impedance log.

The algorithm that will be used in this study is the BLIMP (BandLimited IMPedance inversion) algorithm as described in Ferguson and Margrave (1996). One limitation of that work is that the impedance log was not modified to accommodate any structural variations that were seen in the seismic which caused a horizontal smearing of low frequencies throughout the inversion. This study uses a modified version of the BLIMP algorithm to accommodate for shifts in time due to structure. The following steps have been slightly modified from Ferguson and Margrave (1996) to reduce structure related smearing of the low frequencies:

1. Shift the impedance log in time to accommodate for any structural trend that may be in the seismic.
2. Compute the linear trend of the impedance log and remove it to help reduce edge effects introduced during Fourier domain calculations.
3. Compute the Fourier spectrum of the modified impedance log.
4. Apply a bandlimited integration filter to the seismic trace and then exponentiate the result of the filter. The bandlimited integration filter`s limits are selected by the user.
5. Compute the Fourier spectrum of the integrated and exponentiated seismic trace (4).
6. Determine a scalar that matches the mean power from the spectrum of the impedance log (3) to the spectrum of the integrated seismic trace (5).
7. Multiply the spectrum of the integrated seismic trace by the scalar determined in (6).

8. Apply a low-pass filter to the impedance log spectrum (3) and add to the scaled seismic spectrum (7). The low pass value is selected by the user.
9. Inverse Fourier Transform the result in (8).
10. Add the linear trend that was removed in (2) to generate the completed impedance result.

MODEL DESCRIPTION

To create the model used in this study, well logs were used from the Violet Grove area in west central Alberta. Well 102-07-11-048-09W5 and Well 102-08-14-048-09W5 were combined to form a single log containing well data from the surface to a depth of 2300 m. A linear gradient was applied as the overburden (0 to 308 m) and underburden (2220 to 2300 m) for the P-wave and S-Wave velocity logs. The linear trend was found by fitting a line of best fit through the logged data. For the density log a mean value was used for the overburden and underburden. Well 102-08-14-048-09W5 did not have a shear log so values from 1670 m to 2220 m were calculated using a Vp/Vs ratio of 2. As this is a synthetic experiment the approximation is acceptable as the zone is below the injection interval and the study only inverted the p-wave seismic response. This set of logs then formed the Violet Grove baseline logs and are shown on the left side of Figure 1.

To create the Violet Grove monitor logs, Gassmann fluid substitution from the Cardium to the lower Cardium was used. The Cardium is picked at 1600m and the lower Cardium is picked at 1639m, creating a reservoir interval of about 39m. The mineral matrix was defined as 72% shale and 28% quartz sand with a density of 2607 kg/m^3 and a bulk modulus of 27.0 GPa. The original fluid was taken to be 50% oil and 50% brine, with a density of 878 kg/m^3 and a bulk modulus of 1.7 GPa. 10% CO_2 was then injected such that the replacement fluid contained 45% oil 45% brine 10% CO_2 as it was assumed that the brine and oil would be displaced equally. The replacement fluid had a density of 841 kg/m^3 and a bulk modulus of 1.8 GPa. The rock properties used in this fluid substitution were derived in part from Chen (2007) and the Violet Grove well log data. These values were then used to calculate the substitution using an algorithm in MATLAB based on the Gassmann relation described in Smith et al. (2003). The fluid substituted logs are shown in the right panel of Figure 1.

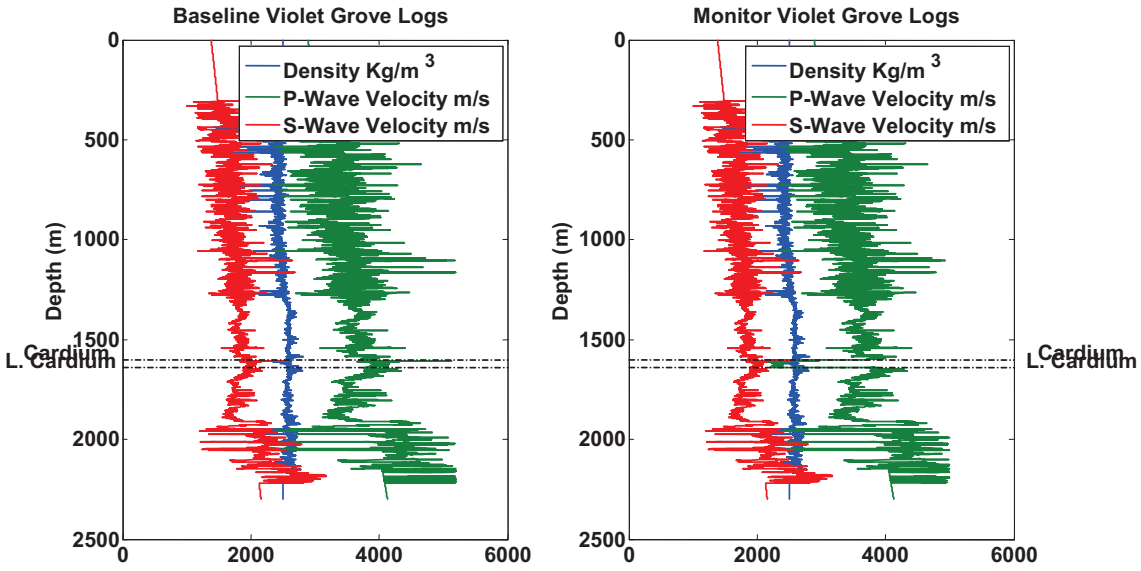

FIG 1: These are the well logs used to make the time-lapse model in this study; blue is the density log, green is the P-wave velocity log and red is the S-wave velocity log. The baseline well logs are in the left panel while the fluid substituted logs are in the panel on the right. The fluid substituted zone is from the Cardium to the Lower Cardium. The p-wave velocity is greatly lowered in this interval after the fluid substitution where as the s-wave velocity and the density are not.

The model was created using LOGSEC (CREWES, 2011), a well log propagation program based in MATLAB. The baseline log was used as the regional log and the monitor log was used for the injection site. The Violet Grove area has predominantly flat horizons (Chen, 2007), however to add a structural complication the model was designed to incorporate a 2.8 degree dip in the reflectors. The injection well is located at the center of the model at 500 m, Figure 2. Logs were propagated using an algorithm that combines the surrounding wells together using a weighting function that is based on the proximity to the propagated log. This allows the injection well signature to be carried away from the well and then taper off at about 100 m from the injection site.

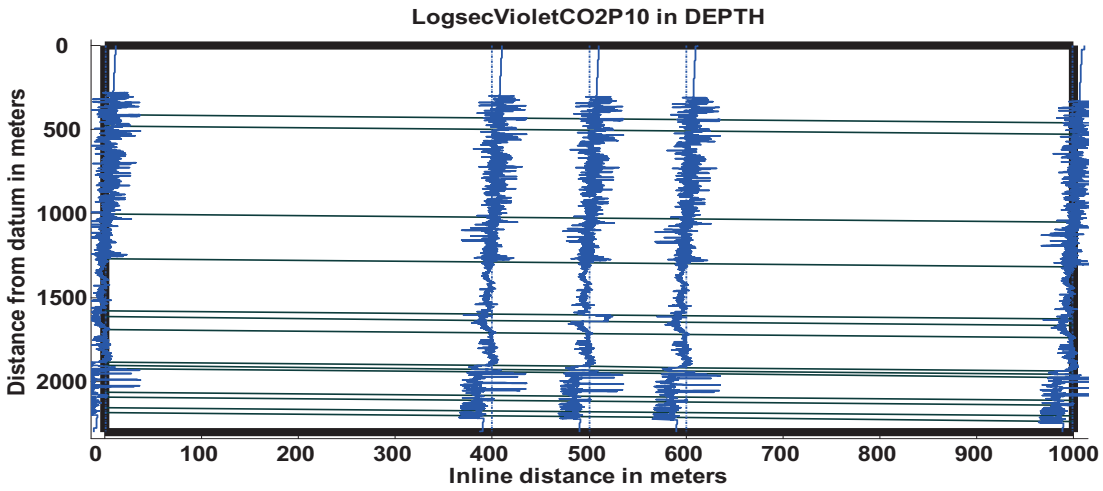

FIG 2: Five logs were placed in the model to define the structure before propagation. The monitor log is located at 500 m. Baseline logs were placed at 400 and 600 m to limit the extent of the carbon-dioxide propagation. Baseline logs were placed at 0 and 1000 m for structural constraints.

The seismic data (Figure 3) was produced by calculating normal incidence seismograms from the propagated well sections. Reflectivity was calculated from the impedance logs and then convolved with a zero phase wavelet seen in Figure 4.

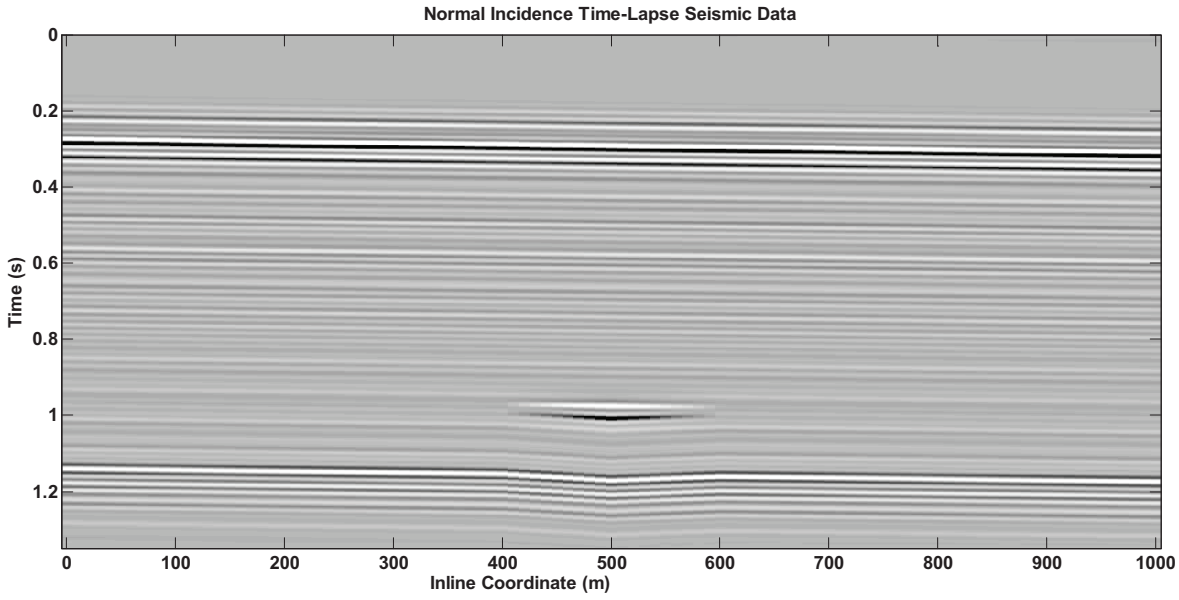

FIG 3: The normal incidence time-lapse seismic data, shown here, was produced using LOGSEC. Note the fluid injection zone at about 1 second and 400 to 600 m inline.

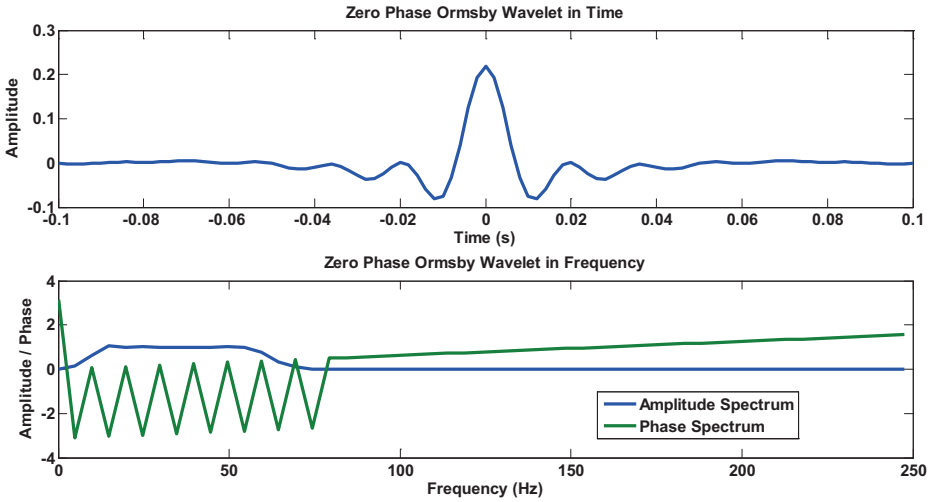

FIG 4: This zero-phase Ormsby wavelet was convolved with the reflectivity calculated from the propagated logs. The upper panel shows the wavelet in time where as the bottom panel shows the frequency spectrum of the wavelet, where the amplitude spectrum is the blue curve and the green curve represents the phase spectrum.

Results

Initial Experimentation

As this is a synthetic experiment, the true impedance values are available to allow absolute error analysis. To compare the true impedance to the inversion results the true impedance needed to be resampled in time and needed to be filtered (Figure 5). A low-pass frequency filter was applied that removed frequencies that were higher than 85 Hz. This was to remove the high frequency variations in the data that was observed in the true impedance and not in the seismic data such that a better comparison could be made. To keep the inversions consistent a high frequency cut-off of 85 Hz was also selected when computing the inversion.

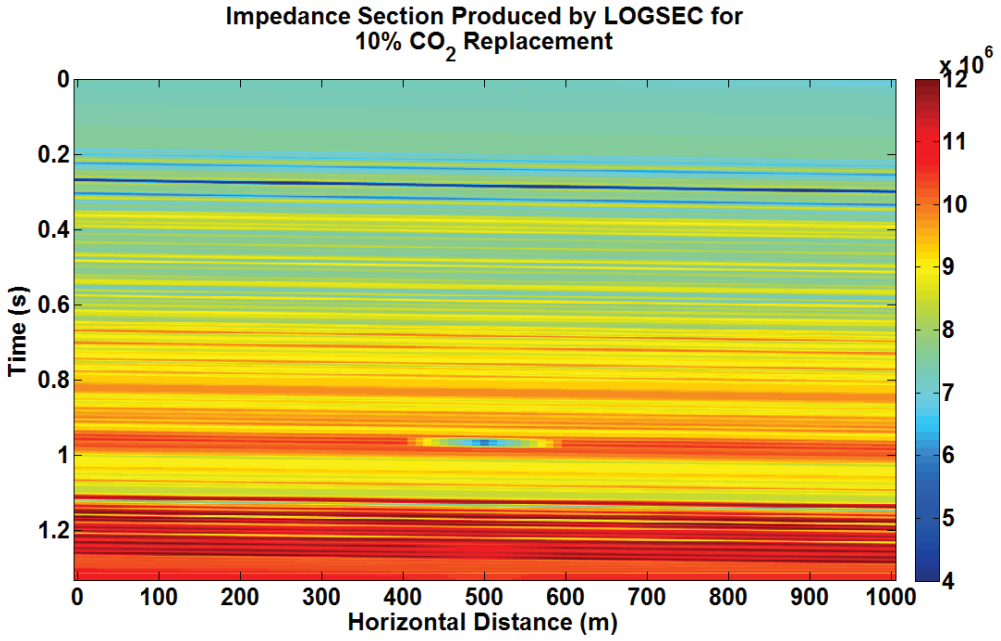

FIG 5: The filtered and resampled true impedance result calculated in LOGSEC with the impedance logs.

For a starting point, a low frequency cut off value was chosen as 10 Hz as that is the value used by McCrank (2009) in the Ardley Flats inversion example. Figure 6 shows the inversion result when the baseline log is used and Figure 7 shows the inversion result generated when the time-lapse log is used. Looking at these figures it can be seen that the baseline log does a good job of estimating the regional data but overestimates the impedance for the injection region. The monitor log on the other hand, underestimates the impedance at the injection site but also underestimates the regional data, which can be seen by the blue color that cuts across the section at about 1 second. Figure 8 and Figure 9 show the error between the true impedance result and the baseline inversion and the true impedance result and the time-lapse inversion respectively. The error is very high (120%) in some places due to the lack of correlation between the filtered true impedance and the inversion results. Most of these high errors are associated with the coal zones that are located at about 0.2-0.4 seconds and are not attributed with the injection zone. The baseline inversion has errors of about -80% at the injection site where as the monitor inversion only has an error of about 40% at the injection site. This shows promise that the monitor log produces a better result when inverting time-lapse data.

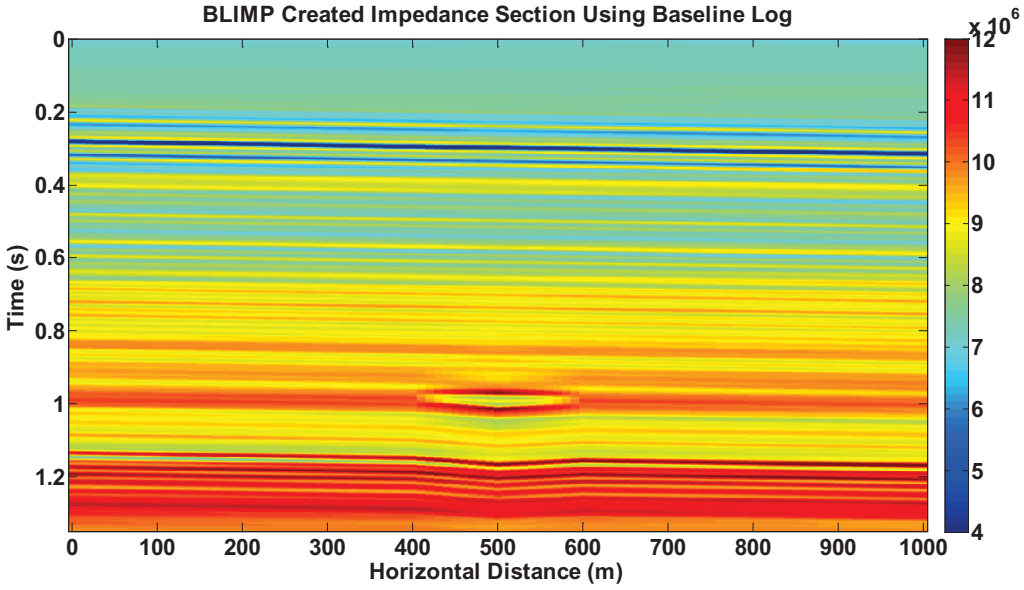

FIG 6: The inversion result using the baseline log with a low frequency cut-off of 10 Hz and a high frequency cut-off of 85 Hz.

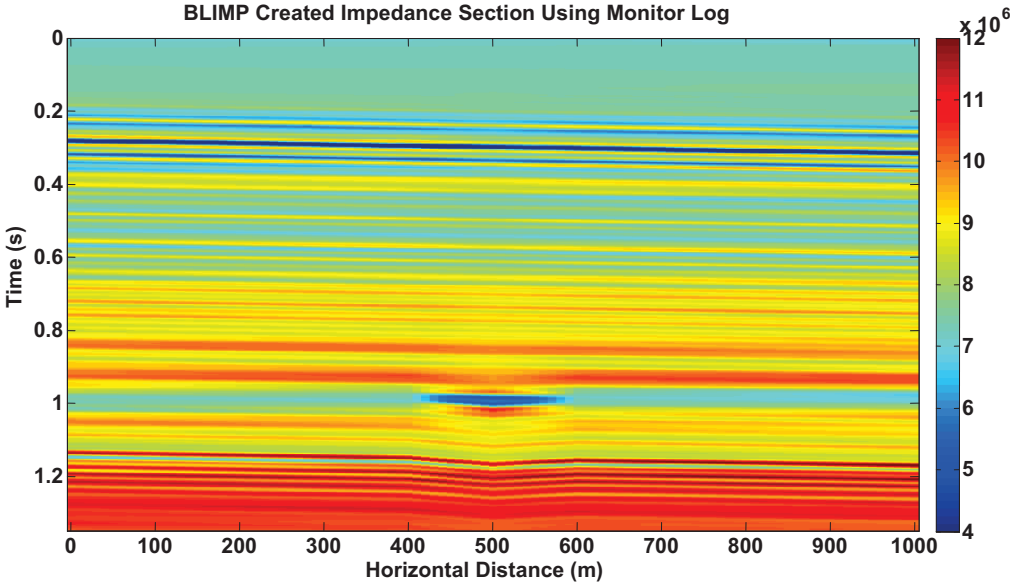

FIG 7: The inversion result using the monitor log with a low frequency cut-off of 10 Hz and a high frequency cut-off of 85 Hz.

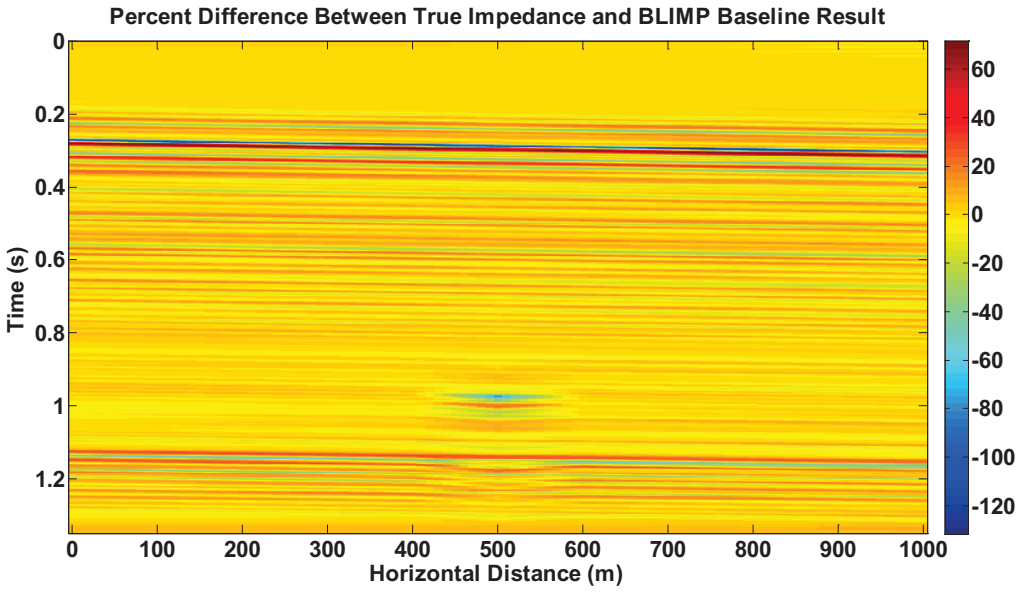

FIG 8: The percent difference between the true impedance and the baseline Inversion result. The low frequency cut-off is 10 Hz and the high frequency cut-off is 85 Hz.

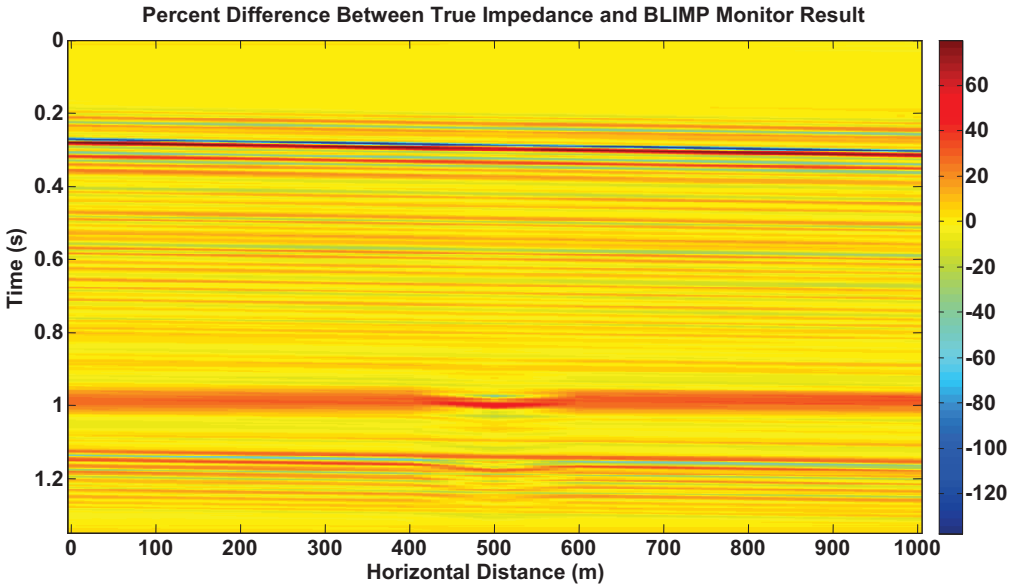

FIG 9: The percent difference between the true impedance and the monitor inversion. The low frequency cut-off is 10 Hz and the high frequency cut-off is 85 Hz. Note the smearing in the data follows a horizontal trend and not the trend of the structure.

Another obvious problem that can be seen in especially Figure 9 is a horizontal trend to the errors. This trend can be attributed to the low frequency well information being smeared across the impedance section. The horizontal nature of this smearing can be corrected for by adding a structural model into the inversion. This has been done by picking a horizon for the inversion to follow. The first step is to calculate the time that

the log goes through that horizon at its lateral location and then shifting it in time accordingly along the horizon. This has been done for the monitor log inversion and can be seen in Figure 10. The error between the true impedance and the monitor inversion with the horizon time adjustment can be seen in Figure 11. The low-frequency smearing now has the same trend as the structure of the data. Figure 12 shows a difference plot between the time-lapse inversion and the time-lapse inversion with the horizon time adjustment. This shows that there is up to 15% error in this model that can be attributed for the lack of structural input in the inversion. Unless the model is flat horizons it is essential that a structural input be used in bandlimited impedance inversion to produce the most accurate results.

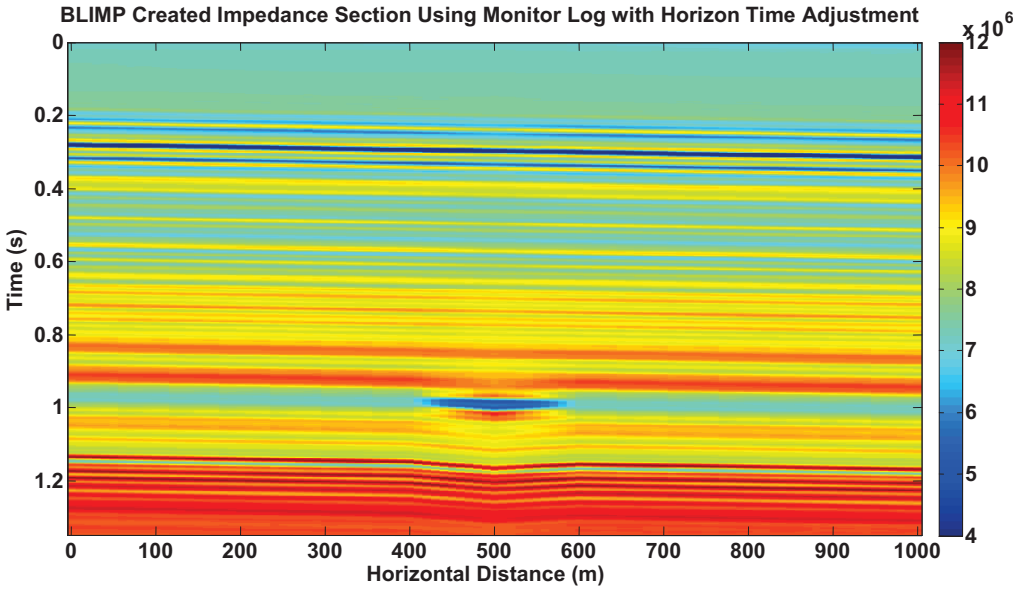

FIG 10: The inversion result using Time-Lapse log and applying the horizon time adjustment using a low frequency cut-off of 10 Hz and a high frequency cut-off of 85 Hz.

While the horizon time adjustment did account for the trend of the smearing, its amplitude is still is strongly evident in the section. While we do expect some smearing, the ideal situation would be to minimize this effect so the seismic data is contributing more than the impedance log. This effect is mostly based on the low frequency limit that is chosen and will be investigated further in the next section.

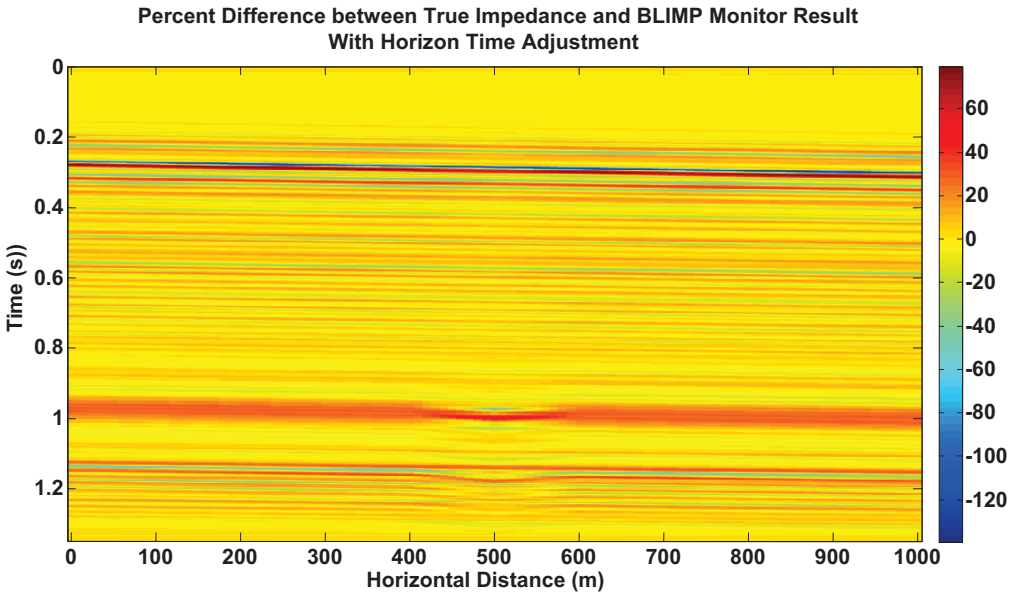

FIG 11: The percent difference between the true impedance and the monitor inversion result with the horizon time adjustment. The low frequency cut-off is 10 Hz and the high frequency cut-off is 85 Hz. Note the smearing of the data follows the structure not a horizontal trend.

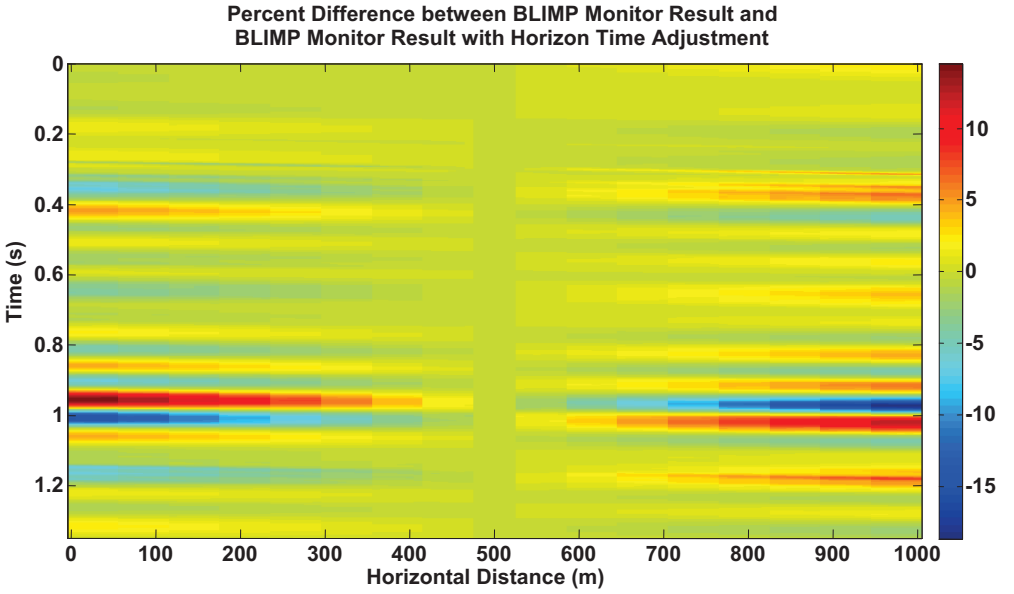

FIG 12: The percent difference between monitor inversion result with no horizon adjustment and the monitor inversion result with a horizon time adjustment. Note the symmetrical behaviour of the error due to the dipping trend of the structure.

Frequency Study

To help identify the best low-frequency cut-off, various low-pass filters were applied to the baseline impedance log, the monitor log, and the integrated seismic data as seen in Figure 13. It is evident that the two impedance logs start to diverge after 1.5 Hz and have much more separation after 4.5 Hz. The seismic data seems to be following the

impedance trend after about 4.5 Hz and is adding more detail after that point. Looking at these plots it seems that a low frequency cut-off could be selected at about 4.5 Hz. Ideally the low frequency cut-off should be chosen where the integrated seismic tapers off in the low end, such that both the impedance log and the seismic are contributing an equivalent amount of data at that point.

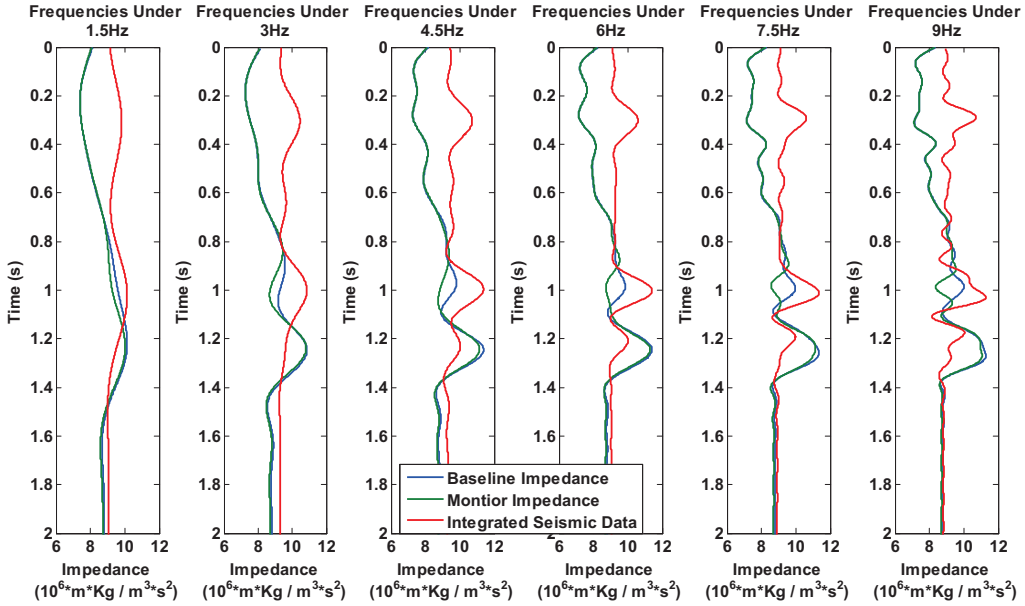

FIG 13: The impedance response for the baseline impedance log (blue), the monitor impedance log (green) and the integrated seismic data (red) when various low-pass frequency filters are applied. Note that the injection zone is at about 1 second.

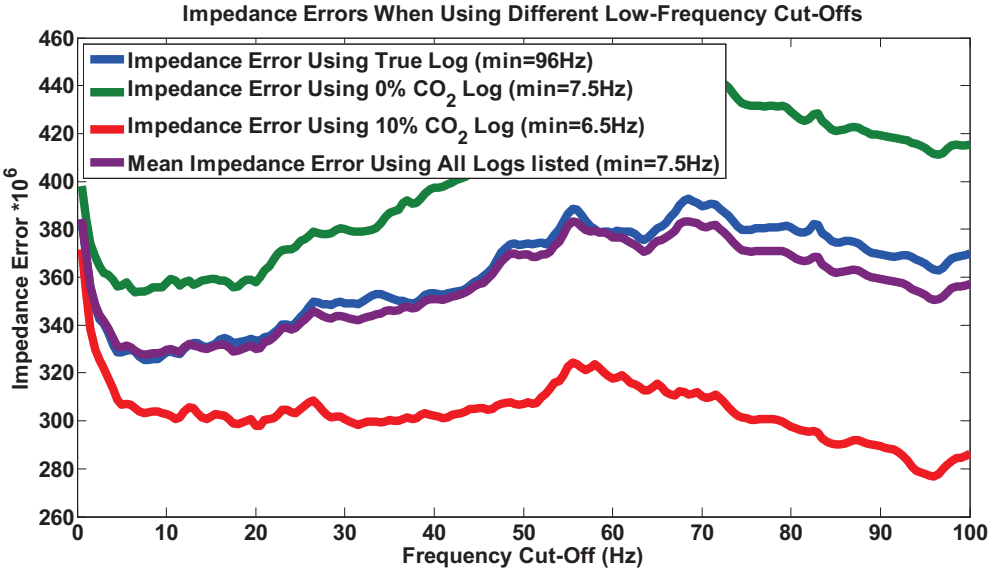

Figure 14: Impedance errors for different low-frequency cut-offs. Blue is the error when the BLIMP inversion is done using the true log. Green is the error when the inversion is done using the baseline log. Red is the error when the inversion is computed with the monitor log. The purple curve is the average of the other curves.

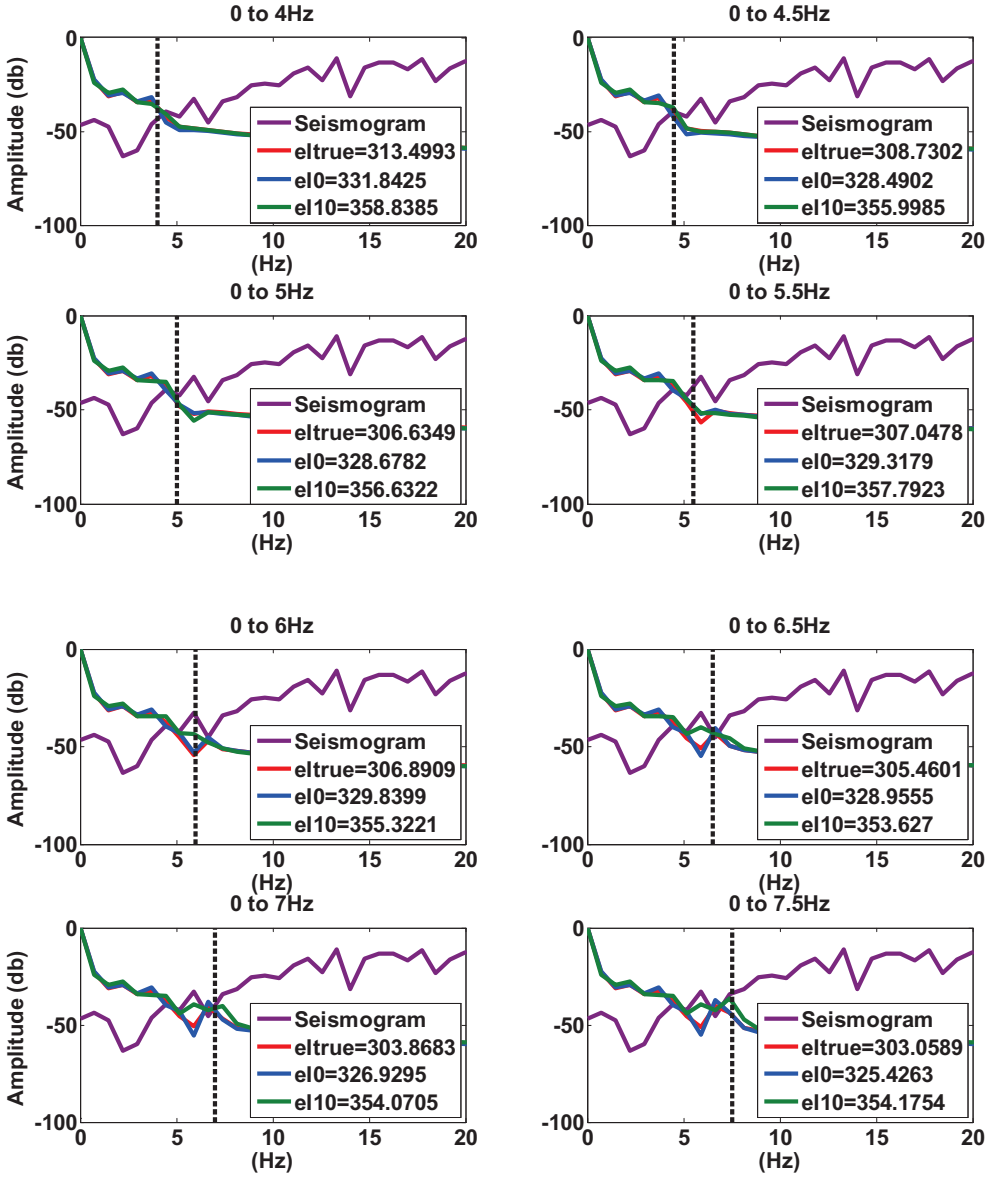

Figure 15: Frequency amplitude plots for different low frequency cut-offs and impedance inversion errors. The purple curve is the amplitude spectrum of the seismogram. The red curves are the low-pass filtered true impedance log where the filter band is indicated in the title of the plot. The blue curves are the low-pass filtered baseline impedance log for various filter bands. The green curves are the low-pass filtered monitor impedance log for the specified frequency band. The errors are the sum of the absolute value of the difference between the BLIMP inversion using the indicated log and the true impedance. These errors need to be multiplied by a factor of 10^6.

Choosing a frequency where the impedance log stops contributing data, also called the low frequency cut-off, is a very important limit. If too much of the impedance log is applied to the data the results are not optimal as the impedance log is adding its own detail to the log not just the trend. If too little of the impedance log is applied to the data then the frequency spectrum becomes notched. Figure 14 shows the error associated when doing a BLIMP inversion with the true impedance and the baseline and monitor

logs for a range of low frequency cut-offs between 0.5Hz and 100Hz. The lowest error for the baseline and monitor logs is between 6.5-7.5 Hz. The lowest error for the true impedance is 96 Hz which is understandable as high cut-offs enable detail from the logs to overwhelm the signal and since it is the solution we would expect the inversion to favour high frequency cut-offs in this case. Figure 15 shows the amplitude spectra for low pass filtered impedance logs with high cut offs ranging from 4 Hz to 7.5 Hz. At a cut-off higher than 5 Hz the impedance logs start add too much of their own detail that appears to be contradictory to the seismic signal. For this study a low-frequency cut-off of 4.5 Hz was chosen.

Final Experimentation Using BLIMP

A BLIMP inversion was computed in MATLAB using the algorithm as described in the Theory section of this paper. The low frequency cut-off was chosen to be 4.5 Hz and the high frequency was chosen as 85 Hz. Both the baseline and monitor impedance inversions had the horizon time adjustment applied, the results for these inversions are seen in Figure 16 and Figure 17, respectively. Figure 18 and Figure 19 show the percent error between the true impedance and the baseline impedance inversion result and the true impedance and the monitor impedance inversion result. The baseline impedance inversion result still does not fully capture the character of the injection zone and has a 28% average error over this zone at 500m. The mean error for the majority of the rest of the section is within ±10% of the true impedance section. The one main exception to this is the coal zone located at about 0.2 to 0.4 seconds. These coals have high reflection coefficients (~0.2-0.3) and therefore are approaching the limit where the logarithmic approximation is still valid, as stated in Equation 4. This may be why there is very high error near these coal beds and not anywhere else in the section. The monitor log only has 23% average error over the injection zone at 500m and again about ±10% error for the remaining section, excluding the coal interval.

To analyze the difference between the baseline and monitor inversions more quantitatively, the impedance errors were summed and synthetic seismograms were computed and compared with the seismic data at the location of the injection well (500 m). To maximize the correlation between the seismic and the synthetic the wavelet was scaled to match the maximum amplitude in the interval between 0.8 and 1.2 seconds. Figure 21 shows the baseline inversion comparison, where the total absolute error of the impedance was 3.5151×10^8, and the maximum cross-correlation between the seismic and the synthetic seismogram was 0.9449. This compares to the monitor inversion (Figure 22), where the total absolute error of the impedance was 3.3003×10^8, and the maximum cross-correlation value was 0.9655. The coal interval was causing large errors to be produced so additional error calculations were conducted, using only the data from times greater than 0.5 seconds. The baseline inversion had 2.4593×10^8 impedance error in this interval and a maximum cross-correlation value of 0.9892, whereas the monitor inversion had an impedance error of 2.0672×10^8 and a maximum cross-correlation of 0.9787. These values show that the monitor impedance inversion has slightly better results than the baseline impedance inversion results at this point.

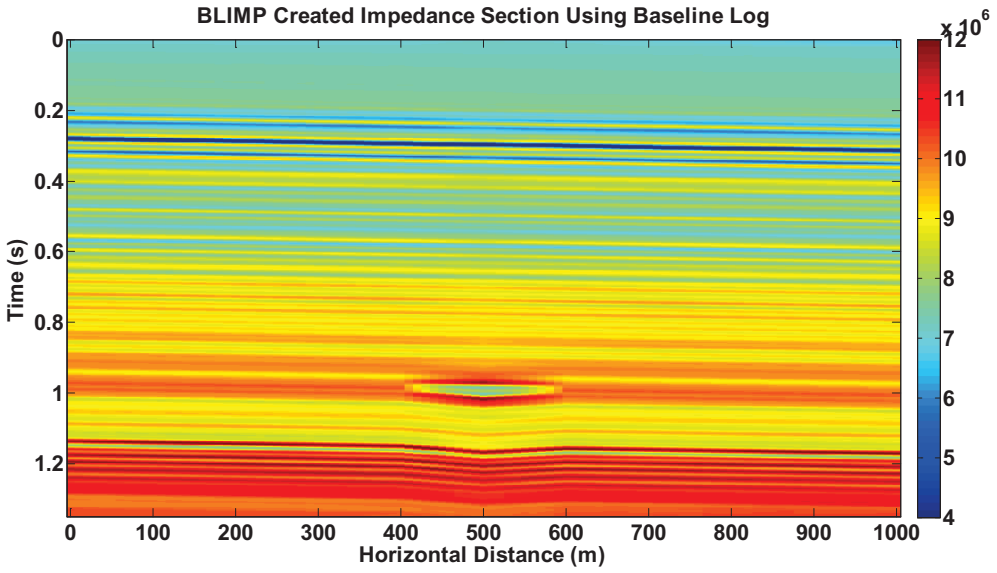

FIG 16: The impedance result using the baseline impedance log with at low frequency cut-off of 4.5 Hz and a high frequency cut-off of 85 Hz.

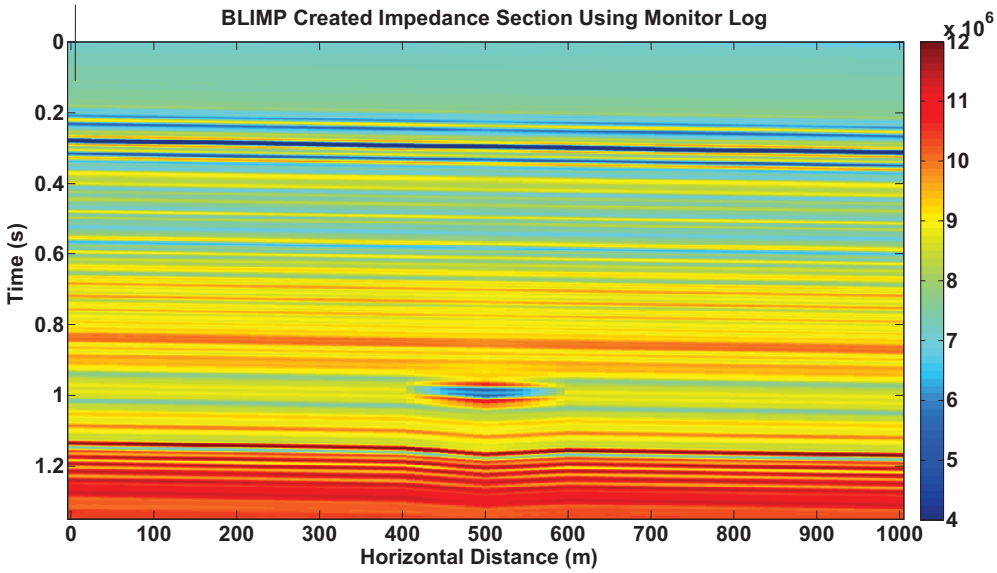

FIG 17: The impedance result using the monitor impedance log with at low frequency cut-off of 4.5 Hz and a high frequency cut-off of 85 Hz.

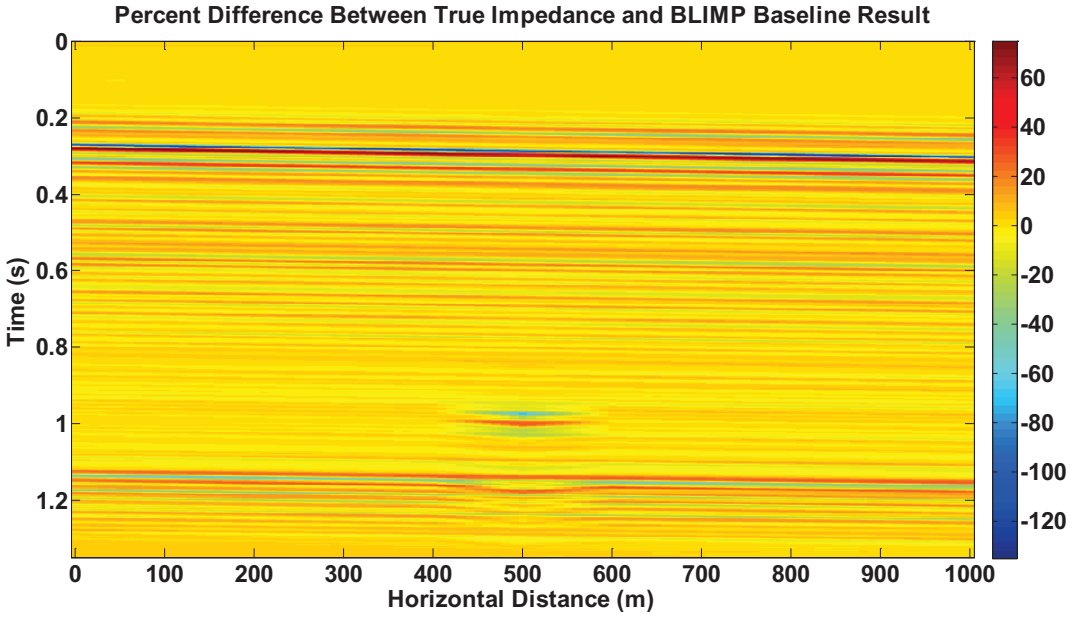

FIG 18: The percent difference between the true impedance and the baseline inversion result for a low frequency cut-off of 4.5 Hz and a high frequency cut-off of 85 Hz. The injection zone is still being under estimated but most of the other error in the section falls within ±10%.

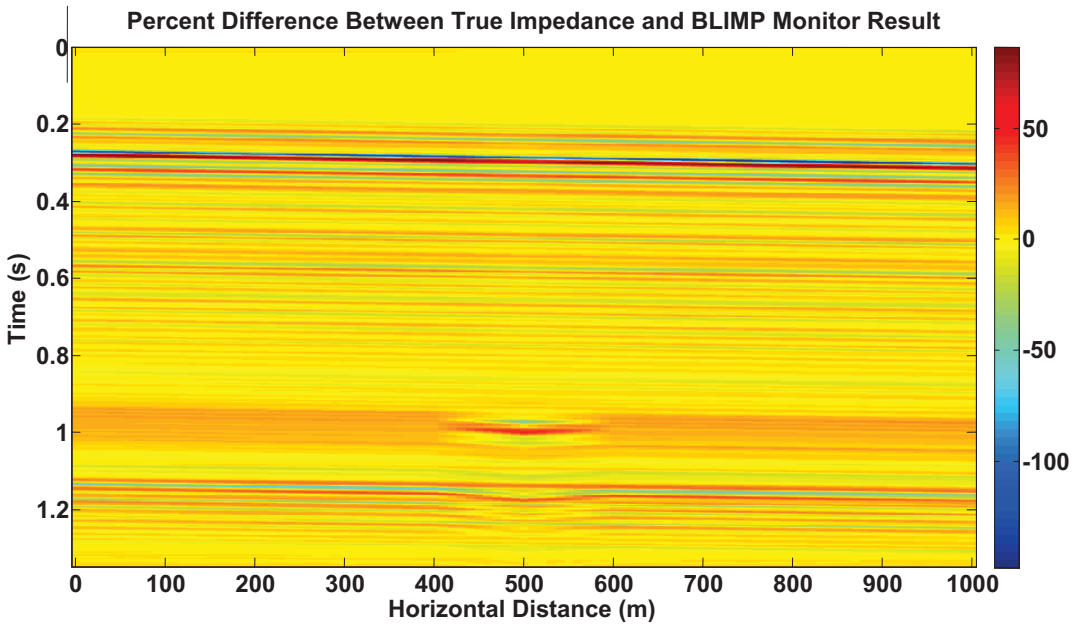

FIG 19: The percent difference between the true impedance and the monitor inversion result for a low frequency cut-off of 4.5 Hz and a high frequency cut-off of 85 Hz. There is still some low frequency leakage that can be seen in the injection interval (~1 s) but is much less than in Figure 11. Most of the regional error, however, falls within ±10%.

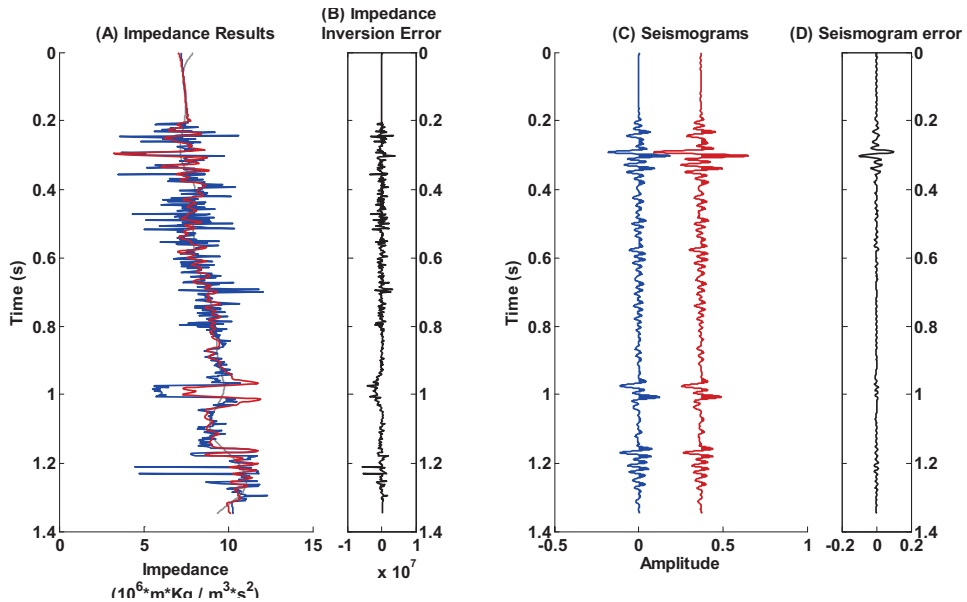

FIG 20: The correlation of the true impedance and the baseline impedance inversion result at the injection site (500 m). In (A) the grey curve is the low impedance log that was supplied by the baseline impedance log. The red curve is the baseline impedance result and the blue curve is the true impedance. In (B) the impedance error between the true impedance and the baseline impedance inversion result; the absolute sum of the error was found to be 3.6151 x 10^8. In (C) the seismograms are compared where the blue curve is the seismic data and the red curve is the synthetic calculated from the baseline impedance inversion result. In (D) the error between the seismograms is shown; the maximum cross correlation between these seismograms was found to be 0.7640.

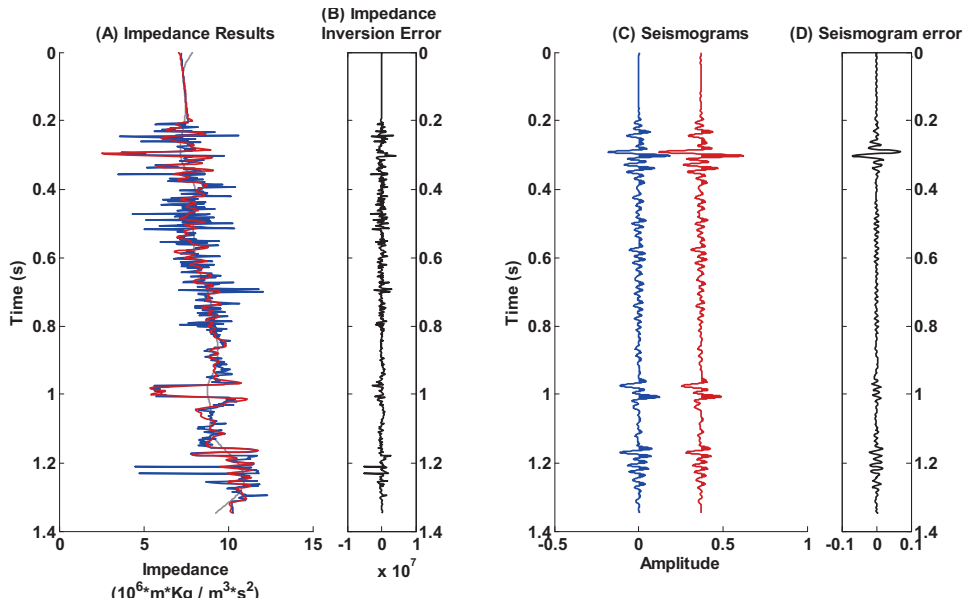

FIG 21: The correlation of the true impedance and the monitor impedance inversion result at the injection site (500 m). In (A) the grey curve is the low impedance log that was supplied by the monitor impedance log. The red curve is the monitor impedance result and the blue curve is the true impedance. In (B) the impedance error between the true impedance and the monitor impedance inversion result; the sum of the error was found to be 3.3003 x 10^8. In (C) the seismograms are compared where the blue curve is the seismic data and the red curve is the

synthetic calculated from the monitor impedance inversion result. In (D) the error between the seismograms is shown; the cross correlation between these seismograms was found to be 0.6754.

Final Experimentation Using Hampson Russell Software

To verify that the result from the BLIMP algoritim was producing accurate inversions when compared to other algorithms, Hampson Russell Software was chosen for this task. Figure 23 shows the Bandlimited impedance results using the Hampson Russell Software algorithm for the Baseline inversion. 4 Hz was used as the low frequency cut-off as decimals were not permitted for this value. Figure 24 shows the percent difference between the Blimp algorithm and the Hampson Russell algorithm for the Baseline inversions. The difference between the different algorithms is within 5% which should verify that the BLIMP algorithm is successful in completing accurate inversions.

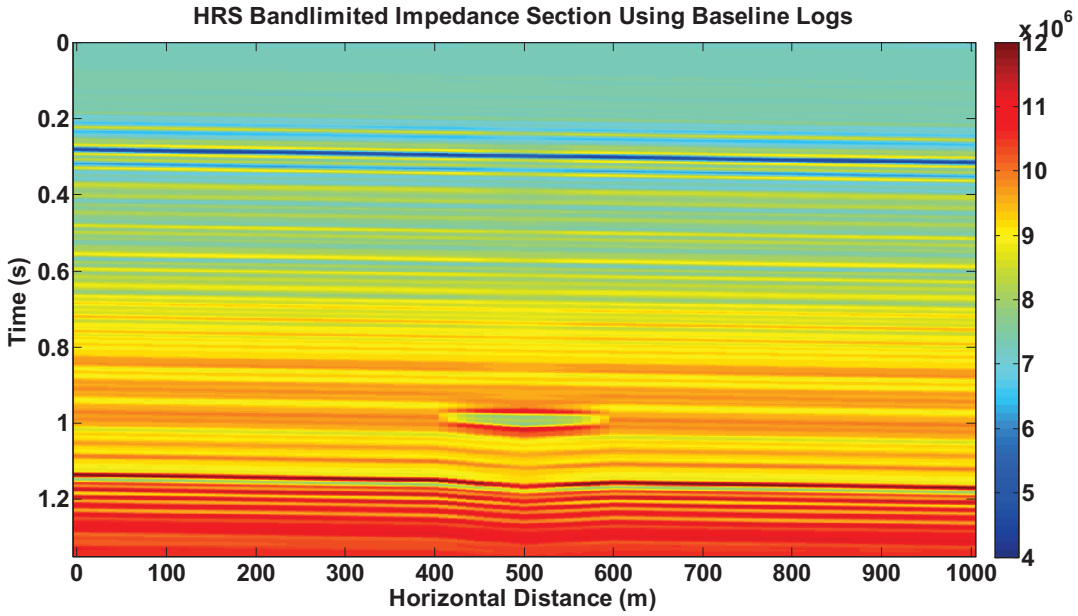

FIG 22: This is the Hampson Russell Software bandlimited inversion result using the baseline impedance log. A 4 Hz low frequency cut-off was used instead of 4.5 as decimals are not permitted in the Hampson Russell Software package.

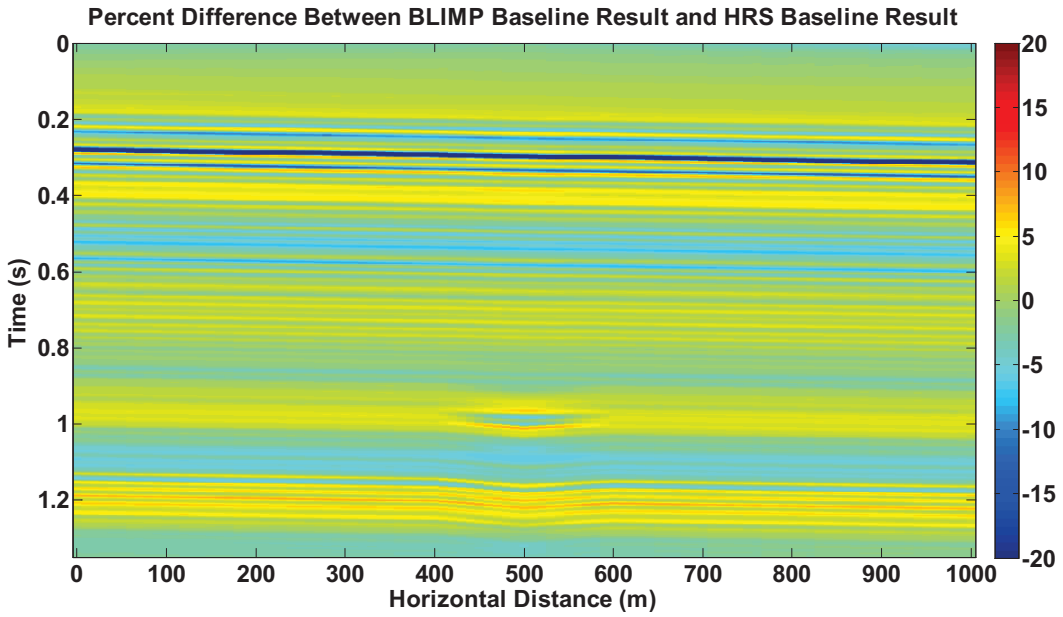

FIG 23: The percent difference was calculated between the MATLAB BLIMP inversion result and the Hampson Russell bandlimited inversion result. Most of the section, excluding the coal region (0.2-0.4 seconds) falls within ± 5% error.

CONCLUSIONS

Several problems became evident when investigating acoustic impedance in a time lapse study. These include the incorporating structure, producing a known impedance section that can be easily compared to the inversion results and choosing the optimum low frequency cut-off. Incorporating the structural trend into the inversion is essential as this creates a bulk time shift that matches the well log with the seismic data. This needs to be further extended to adjust for any disagreements with the well log and the seismic data on a finer scale. This would help reduce the error between the true impedance and the impedance inversion. The true impedance is known but needs to be appropriately formatted to the data to ease the difficulty of interpreting the inversion results. In the Violet Grove example there were coal intervals which created very large error in the section. Creating models that do not have lithologies that cause high reflection coefficients will aid in the better correlation between the known impedance and the impedance inversion.

The low frequency cut-off must be chosen appropriately such that the impedance inversion has a smooth frequency spectrum. Choosing this value too high, produces low frequency smearing across the inversion section and choosing a frequency that is too low, reduces the amount of reliable information at low frequencies. A method for choosing the low frequency cut-off needs to be investigated but using a value of around 5 seems to work for most cases.

It seemed obvious that the monitor well log information would produce a superior inversion when compared to using the baseline well log information. This study has shown that the sum of the absolute difference between the monitor inversion and the true

impedance is lower than the difference between the baseline inversion and the true impedance. The cross correlation between the synthetic seismogram created from the monitor log and the true reflectivity was similar to the cross correlation between the synthetic seismogram created from the baseline log and the true reflectivity. This shows that the inversions are similar with the monitor inversion being slightly more accurate at the injection well site, however for the overall section the best impedance inversion may be to use both logs where the baseline log is used for the regional zone and the monitor log is used for the injection zone to achieve optimal results when completing a time-lapse inversion.

FUTURE WORK

This study was completed with noise free normal incidence synthetic seismic data. The next step will be to study the effects of a time-lapse inversion on noisy data, processed data from synthetic shot records and eventually a real data set. Developing the BLIMP method into a user friendly fully working package will also be pursued.

ACKNOWLEDGMENTS

I would like to thank Don Lawton and Penn West for the use of the Violet Grove data. I would also especially like to thank the CREWES sponsors for their continued financial support and CREWES staff for their guidance.

REFERENCES

Chen, F., 2007, Interpretation of Time-lapse Surface Seismic Data at CO_2 Injection Site, Violet Grove Alberta: Department of Geology and Geophysics, University of Calgary.

CREWES, 2011, CREWES Toolbox for MATLAB: Department of Geoscience, University of Calgary.

Ferguson, R. J. and Margrave, G. F., 1996, A simple algorithm for bandlimited impedance inversion: CREWES Research Report, Vol. 8, No. 21.

Lindseth, R. O., 1979, Synthetic sonic logs – a process for stratigraphic interpretation: Geophysics, Vol. 44, No. 1.

McCrank, M. J., 2009, Seismic Detection and Characterization of a CO_2 Flood in Ardley Coals, Alberta Canada: Department of Geoscience, University of Calgary.

Oldenburg, D. W., Scheuer, T., and Levy, S., 1983, Recovery of the acoustic impedance from reflection seismograms: Geophysics, Vol. 48, No. 10.

Pendrel, J., 2006, Seismic Inversion – Still the best tool for reservoir characterization: CSEG Recorder, Vol. 31, No. 1.

Smith, T. M., Sondergeld, C. H., and Rai, C. S., 2003, Gassmann fluid substitutions: A tutorial: Geophysics, Vol. 68, No. 2.